Intensity profile of the 22° halo

David K. Lynch* and Ptolemy Schwartz†

Hughes Research Laboratories, 3011 Malibu Canyon Road, Malibu, California 90265

Received October, 9, 1984; accepted November 27, 1984

We report the first relative intensity measurements made to our knowledge of the 22° halo, obtained from photographic photometry of a halo of exceptional brightness and uniformity. The maximum brightness occurs at 22.8°, and a relative minimum occurs at 19.7°. The full width at one half the maximum intensity is 3.4°. A low-intensity tail reaches from 29° to 39°.

INTRODUCTION

Despite the growing scientific awareness of ice-crystal halos, there is surprising lack of quantitative observational data about them. Even the most basic (and often-referenced) angular measurements sometimes consist of casual determinations of the radii of circular halos with no mention whatever of the intensity distribution. More-complex halos are reported with either freehand drawings or photographs. Seldom if ever are the photographs measured to ascertain the trajectories of noncircular halos. Intensity measurements are unknown, the closest being a smoothed, uncalibrated photographic density scan across a 22° halo by Bruche and Bruche.[1] Quantitative color measurements do not exist for any halo, and only recently have polarization studies been made by Lynch[2] and Konnen.[3] Most of the growing wealth of information about ice crystal halos is theoretical because naturally occurring halos are short lived, episodic, and seldom occur under the conditions necessary for detailed observation. Still, the most basic properties of halos (intensity versus angular position on the sky) are not quantitatively known.

In this paper we present quantitative measurements of the intensity distribution of the 22° halo.

OBSERVATIONS OF THE 22° HALO

The halo observations reported here were made in Malibu, California, on the evening of December 3, 1979. An exceptionally bright and well-defined 22° halo was observed by moonlight (Fig. 1). Its contrast was very high, and the halo was almost perfectly uniform around its circumference. The cirrostratus clouds showed little texture or anisotropy and covered the sky so evenly that their presence could only be inferred from the halo. The moon was approximately 50° above the horizon. A number of photographs were made on Kodak Plus-X pan film with exposure times ranging between 1 and 10 sec. During this time the moon would have moved no more than 0.04°, an insignificant amount compared with the diameter of the moon (0.5°) and with the width of the halos (≃3°). The images of the moon and the halo were carefully centered in the frame to render any image distortion symmetric on the film and to prevent lens ghosts from falling on the halo proper. The following day several exposures of calibrated intensity wedges and grids were made with the same equipment, thereby calibrating intensity on the film and the angular scale and distortion of the 16-mm lens. A scientific laboratory developed the film according to the manufacturer's instructions.

The images of the halo and calibration wedge were digitized using a spot size of 25 μm (0.18°). After the photographic density was converted to true relative intensity (Figs. 2A and 2B), the computerized image was measured to locate the moon, the assumed center of the halo. The location of each pixel (deviation angle D relative to the moon) was calculated, and the entire upper half of the two-dimensional image (approximately 113,000 data points) was reduced to a plot of relative intensity versus deviation angle (angle on the sky) along with an average curve calculated by summing intensity pixels in 0.1° window intervals (Fig. 2C; Table 1, column 1). In reducing the data to a plot of brightness versus angle we assumed that there was no azimuthal variation in brightness based on the comparison of several radial intensity profiles. The lower half of the halo was not used owing to concerns about absorption by the large air mass at large zenith distances.

If there were no halo present, scattering by air molecules and cloud particles would result in a brightness distribution that decreased monotonically away from the moon. In order to remove this background trend we assumed that the halo intensity distribution was independent of the background and represented an additive component to the sky brightness. Since the halo is not expected to contribute light at angles outside its minimum and maximum deviation angles (21.8° and 43.5°, respectively, for no internal reflections in the crystal), we fitted a third-order polynomial to these parts of the intensity distribution and subtracted it from the curve (Fig. 2C). The fit was extended from 15° (the maximum extent of lens flare on the image) to 45°, the maximum sky angle on the film excluding the halo regions between 21.8° and 43.5°. The result is shown in Fig. 2D and should represent the residual halo scattering intensity as a function of deviation angle D measured from the light source. For ease of comparison with this and other theories and observations, Table 1 lists the raw and subtracted normalized intensity distribution for the 22° halo shown in Fig. 1. The effect of misjudging the position of the true background is to shift the curve (Fig. 2D; Table 1, column 3) up or down by a small constant amount and has the greatest effect far out in the profile (>28°). The effect on the values near minimum deviation (≃22°) is small.

The observed intensity profile (Fig. 2; Table 1, column 2) shows a minimum centered at 19.7°. Both observed and

0740-3232/85/040584-06$02.00

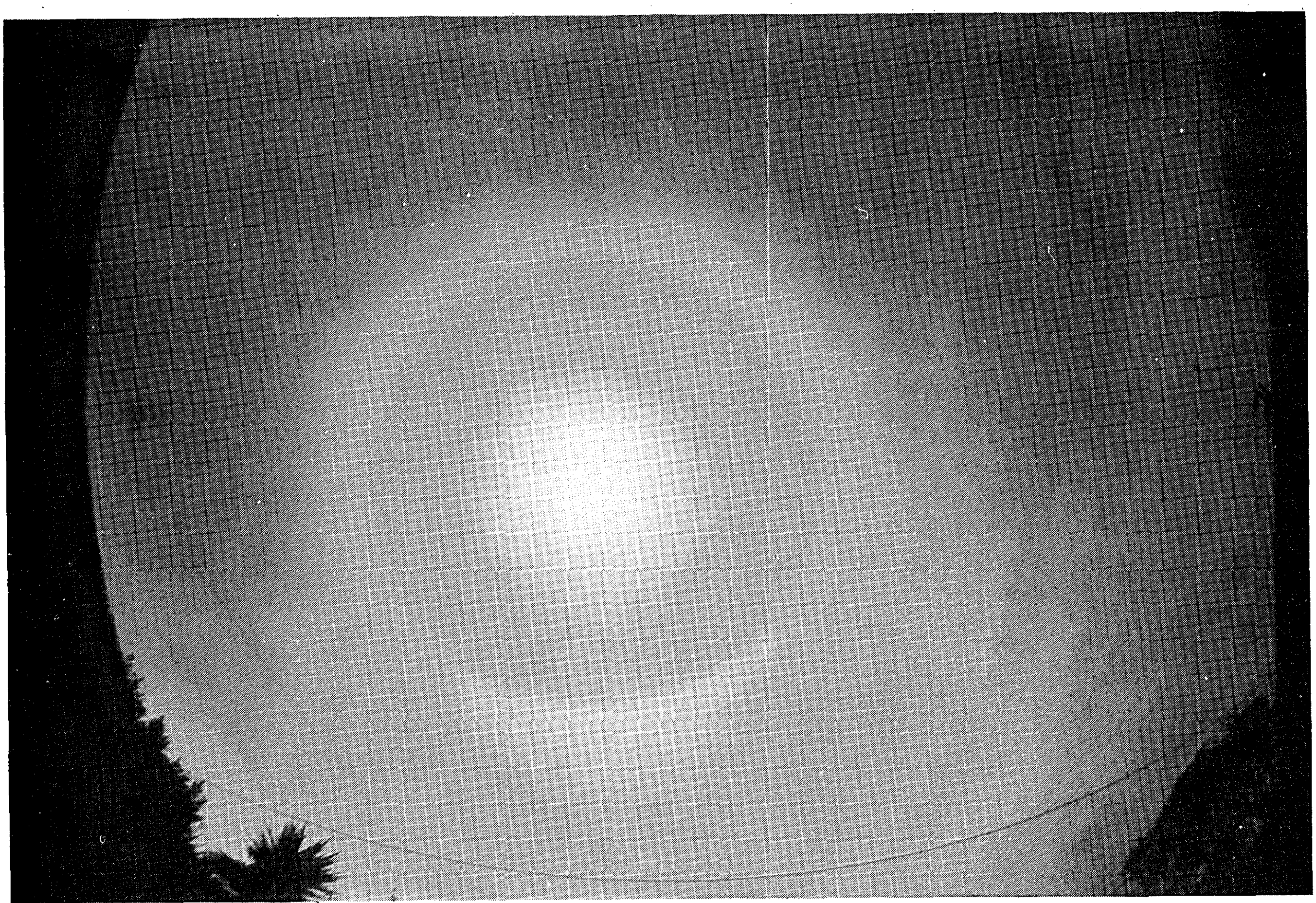

Fig. 1. 22° halo observed on December 3, 1979, in Malibu, California, by the author. The halo was remarkable for its brightness, high contrast, and azimuthal uniformity and because the lunar altitude was about 50°, well above the radius of the halo. No other halos were observed during the display, and the cirrus clouds were uniform and showed virtually no structure or anisotropy.

corrected profiles show a halo brightness maximum at 22.8°, in good agreement with simple minimum-deviation calculations and more-sophisticated theoretical models. The full width at one half of the maximum intensity (FWHM) is 3.4°. A broad tail occurs between about 29° and 39°.

DISCUSSION

The simplest models of the 22° halo that include the finite width of the sun and the dispersion of light in ice predict a FWHM of the radial profile of 2.5°,[4] considerably narrower than our observed profile. If the discrepancy is due to diffraction by the ice crystals (an effect not included in model calculations), we can estimate the size of the crystal responsible for this halo. The diffraction pattern for a slit of width a is given by

$$(I/I_0) = (\sin \alpha/\alpha)^2$$

where

$$\alpha = (\pi a/\lambda)\sin(\theta),$$

where θ is the diffraction angle, λ is the wavelength, and a is the diffraction aperture width. The half-power widths (FWHM) occur when $\alpha = 1.40$. Using $\lambda = 0.5\ \mu\text{m}$ and $\sin\theta = \theta$, we find a simple expression for the width W_{dif} of the diffraction pattern's first maximum of

$$W_{\text{dif}} = 25.5/a,$$

where W_{dif} is measured in degrees. Since the observed intensity profile is not highly asymmetric, we may estimate the diffraction width W_{dif} of the halo by deconvolving the theoretical width W_{th} from the observed width W_{obs} using the quadrature rule for deconvoluting Gaussians, i.e.,

$$(W_{\text{obs}})^2 = (W_{\text{th}})^2 + (W_{\text{dif}})^2,$$

resulting in $W_{\text{dif}} \simeq 2.5°$ and $a \simeq 10\ \mu\text{m}$. This is only a rough estimate (±30%) because projection effects, index-of-refraction variations, etc. have not been included. The value of a is clearly in the size range for crystals that are expected to be randomly oriented (Nikiforova *et al.*[5])

Since no 46° halo was observed during the December 3, 1979, display we might suppose that the aspect ratio of the crystal was much greater than 1, i.e., the cirrus clouds were composed primarily of columns rather than of plates (Lynch,[4] Pattlock and Trankle[6]). It is also possible that any hexagonal ice crystal without basal pinacoids could cause the 22° halo but not the 46° halo. The most likely candidate are pyramidally terminated bullet crystals.

The profile information reported here is for only one halo, a halo that was not necessarily characteristic of all halos. Indeed, its exceptional brightness may have been due not simply to a larger-than-usual number of scattering crystals

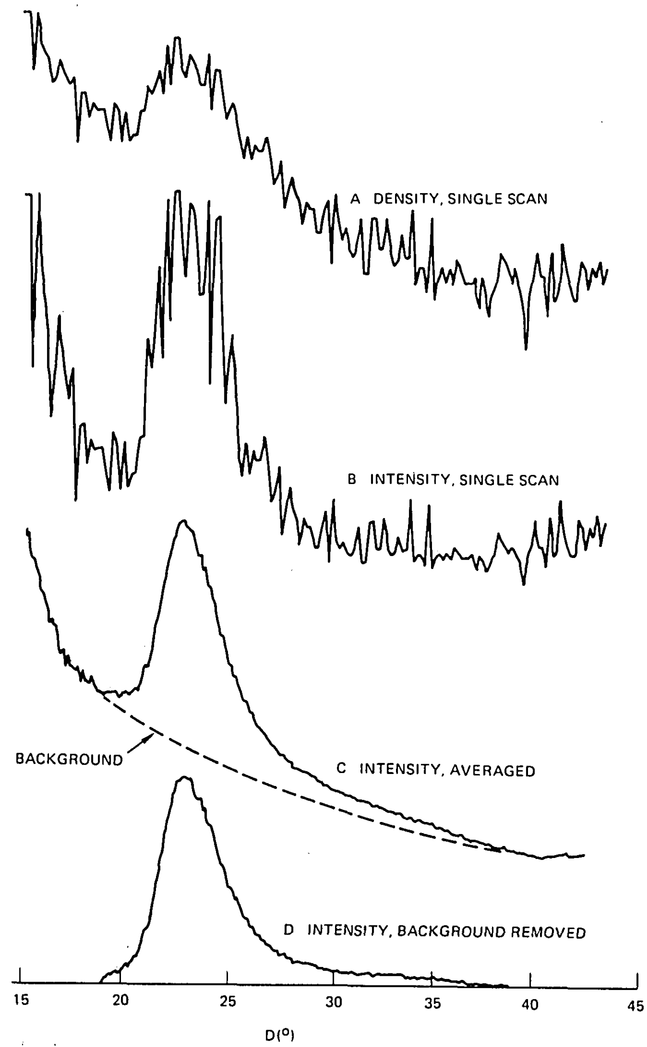

Fig. 2. Reduction of raw data to intensity profile of the 22° halo. A, Photographic density profile for a single vertical scan through the halo and the moon. B, Same scan as A after conversion to relative intensity. C, Averaged intensity profile using approximately 113,000 points. D, Averaged intensity profile after removal of the background trend indicated in C.

but rather to a distribution of crystals (or other effects) that not only rendered the halo bright but also caused its intensity distribution to be different from that of other 22° halos. Although we do not believe that this is likely, only further photometric measurements of other halos can settle the question.

SUMMMARY AND CONCLUSIONS

We have made the first reported photometric measurements of an ice-crystal halo and compared the radial intensity profile with a first-order theoretical model for light refracted and diffracted through the crystal in the plane perpendicular to the refracting edge. The difference between observed and theoretical full widths of the halos suggested that diffraction by crystals approximately 10 μm across their refracting faces widens the halo. Since the 46° halo was not observed, the crystals responsible for the halo reported here were probably

Table 1. Photometric Measurements of the Radial Halo Profile

D (°)[a]	I_{rel}[b]	I_{halo}[c]
15.0	4.80	0.000
15.1	3.15	0.000
15.2	3.17	0.000
15.3	3.07	0.000
15.4	3.03	0.000
15.5	3.04	0.000
15.6	3.00	0.000
15.7	2.96	0.000
15.8	2.89	0.000
15.9	2.87	0.000
16.0	2.86	0.000
16.1	2.82	0.000
16.2	2.78	0.000
16.3	2.72	0.000
16.4	2.75	0.000
16.5	2.71	0.000
16.6	2.70	0.000
16.7	2.63	0.000
16.8	2.57	0.000
16.9	2.59	0.000
17.0	2.59	0.000
17.1	2.52	0.000
17.2	2.57	0.000
17.3	2.51	0.000
17.4	2.51	0.000
17.5	2.50	0.000
17.6	2.49	0.000
17.7	2.51	0.000
17.8	2.44	0.000
17.9	2.50	0.000
18.0	2.46	0.000
18.1	2.44	0.000
18.2	2.44	0.000
18.3	2.42	0.000
18.4	2.46	0.000
18.5	2.42	0.000
18.6	2.39	0.000
18.7	2.39	0.000
18.9	2.38	0.000
19.0	2.38	0.022
19.1	2.39	0.041
19.2	2.39	0.040
19.3	2.40	0.056
19.4	2.39	0.052
19.5	2.39	0.059
19.6	2.40	0.071
19.7	2.37	0.051
19.8	2.38	0.068
19.9	2.38	0.076
20.0	2.40	0.094
20.1	2.40	0.105
20.2	2.38	0.094
20.3	2.39	0.110
20.4	2.40	0.123
20.5	2.42	0.142
20.6	2.41	0.139
20.7	2.43	0.166
20.8	2.48	0.218
20.9	2.53	0.268
21.0	2.52	0.264
21.1	2.52	0.273
21.2	2.57	0.322
21.3	2.65	0.400

Table 1. Continued

D (°)[a]	I_{rel}[b]	I_{halo}[c]	D (°)[a]	I_{rel}[b]	I_{halo}[c]
21.4	2.69	0.448	27.8	2.10	0.154
21.5	2.75	0.507	27.9	2.08	0.138
21.6	2.81	0.568	28.0	2.07	0.129
21.7	2.85	0.611	28.1	2.07	0.131
21.8	2.94	0.692	28.2	2.06	0.127
21.9	2.97	0.728	28.3	2.03	0.105
22.0	3.03	0.790	28.4	2.04	0.118
22.1	3.07	0.834	28.5	2.03	0.114
22.2	3.14	0.904	28.6	2.03	0.111
22.3	3.16	0.924	28.7	2.02	0.109
22.4	3.21	0.979	28.8	2.02	0.108
22.5	3.23	0.980	28.9	2.02	0.113
22.6	3.20	0.981	29.0	2.01	0.108
22.7	3.27	0.997	29.1	2.01	0.109
22.8	3.21	1.000	29.2	1.99	0.098
22.9	3.21	0.998	29.3	1.99	0.101
23.0	3.19	0.986	29.4	1.98	0.094
23.1	3.19	0.991	29.5	1.97	0.086
23.2	3.17	0.972	29.6	1.97	0.089
23.3	3.11	0.925	29.7	1.97	0.090
23.4	3.08	0.897	29.8	1.95	0.075
23.5	3.06	0.886	29.9	1.96	0.089
23.6	3.07	0.902	30.0	1.95	0.076
23.7	2.99	0.831	30.1	1.94	0.073
23.8	3.01	0.852	30.2	1.94	0.075
23.9	2.93	0.782	30.3	1.93	0.070
24.0	2.91	0.766	30.4	1.93	0.074
24.1	2.90	0.763	30.5	1.92	0.068
24.2	2.86	0.731	30.6	1.92	0.065
24.3	2.82	0.697	30.7	1.92	0.070
24.4	2.78	0.659	30.8	1.91	0.067
24.5	2.72	0.608	30.9	1.90	0.062
24.6	2.68	0.574	31.0	1.91	0.066
24.7	2.67	0.572	31.1	1.90	0.067
24.8	2.63	0.542	31.2	1.90	0.070
24.9	2.58	0.493	31.3	1.89	0.063
25.0	2.54	0.463	31.4	1.89	0.065
25.1	2.54	0.463	31.5	1.89	0.062
25.2	2.52	0.455	31.6	1.88	0.057
25.3	2.47	0.407	31.7	1.88	0.060
25.4	2.48	0.420	31.8	1.87	0.058
25.5	2.43	0.376	31.9	1.87	0.061
25.6	2.41	0.363	32.0	1.88	0.066
25.7	2.38	0.343	32.1	1.87	0.062
25.8	2.36	0.324	32.2	1.85	0.050
25.9	2.36	0.327	32.3	1.86	0.057
26.0	2.33	0.307	32.4	1.86	0.065
26.1	2.30	0.284	32.5	1.85	0.056
26.2	2.30	0.284	32.6	1.85	0.063
26.3	2.27	0.260	32.7	1.84	0.055
26.4	2.25	0.245	32.8	1.84	0.054
26.5	2.24	0.240	32.9	1.84	0.056
26.6	2.23	0.234	33.0	1.83	0.052
26.7	2.21	0.217	33.1	1.83	0.058
26.8	2.20	0.215	33.2	1.83	0.053
26.9	2.18	0.197	33.3	1.83	0.056
27.0	2.17	0.196	33.4	1.82	0.053
27.1	2.16	0.187	33.5	1.82	0.055
27.2	2.14	0.174	33.6	1.82	0.061
27.3	2.13	0.168	33.7	1.80	0.042
27.4	2.13	0.169	33.8	1.81	0.053
27.5	2.10	0.145	33.9	1.79	0.038
27.6	2.10	0.145	34.0	1.81	0.052
27.7	2.10	0.150	34.1	1.80	0.052

continued overleaf

Table 1. Continued

D (°)[a]	I_{rel}[b]	I_{halo}[c]	D (°)[a]	I_{rel}[b]	I_{halo}[c]
34.2	1.80	0.047	39.7	1.63	0.000
34.3	1.78	0.036	39.8	1.63	0.000
34.4	1.79	0.042	39.9	1.63	0.000
34.5	1.79	0.050	40.0	1.62	0.000
34.6	1.79	0.048	40.1	1.64	0.000
34.7	1.78	0.044	40.2	1.63	0.000
34.8	1.77	0.040	40.3	1.62	0.000
34.9	1.77	0.044	40.4	1.62	0.000
35.0	1.77	0.039	40.5	1.62	0.000
35.1	1.78	0.053	40.6	1.63	0.000
35.2	1.76	0.032	40.7	1.63	0.000
35.3	1.75	0.030	40.8	1.62	0.000
35.4	1.75	0.035	40.9	1.63	0.000
35.5	1.76	0.041	41.0	1.61	0.000
35.6	1.75	0.035	41.1	1.62	0.000
35.7	1.74	0.029	41.2	1.62	0.000
35.8	1.75	0.038	41.3	1.63	0.000
35.9	1.74	0.031	41.4	1.63	0.000
36.0	1.73	0.020	41.5	1.63	0.000
36.1	1.73	0.024	41.6	1.65	0.000
36.2	1.73	0.025	41.7	1.62	0.000
36.3	1.72	0.021	41.8	1.64	0.000
36.4	1.71	0.017	41.9	1.62	0.000
36.5	1.73	0.036	42.0	1.63	0.000
36.6	1.72	0.024	42.1	1.63	0.000
36.7	1.71	0.014	42.2	1.64	0.000
36.8	1.70	0.010	42.3	1.65	0.000
36.9	1.70	0.015	42.4	1.64	0.000
37.0	1.70	0.009	42.5	1.64	0.000
37.1	1.71	0.022	42.6	1.63	0.000
37.2	1.70	0.015	42.7	1.65	0.000
37.3	1.70	0.016	42.8	1.65	0.000
37.4	1.69	0.015	42.9	1.65	0.000
37.5	1.69	0.012	43.0	1.65	0.000
37.6	1.69	0.015	43.1	1.64	0.000
37.7	1.68	0.005	43.2	1.68	0.000
37.8	1.69	0.019	43.3	1.66	0.000
37.9	1.68	0.011	43.4	1.65	0.000
38.0	1.66	0.000	43.5	1.65	0.000
38.1	1.67	0.009	43.6	1.64	0.000
38.2	1.67	0.010	43.7	1.63	0.000
38.3	1.67	0.010	43.8	1.63	0.000
38.4	1.66	0.000	43.9	1.64	0.000
38.5	1.66	0.007	44.0	1.63	0.000
38.6	1.67	0.017	44.1	1.63	0.000
38.7	1.66	0.007	44.2	1.63	0.000
38.8	1.65	0.004	44.3	1.63	0.000
38.9	1.65	0.001	44.4	1.63	0.000
39.0	1.65	0.000	44.5	1.63	0.000
39.1	1.64	0.000	44.6	1.63	0.000
39.2	1.64	0.000	44.7	1.62	0.000
39.3	1.63	0.000	44.8	1.62	0.000
39.4	1.65	0.000	44.9	1.62	0.000
39.5	1.63	0.000	45.0	1.61	0.000
39.6	1.64	0.000			

[a] Deviation angle D on sky measured from the moon.
[b] Relative intensity of the sky brightness before removal of background (Fig. 2C).
[c] Normalized intensity of profile of the 22° halo with the background removed (Fig. 2D).

randomly oriented columns or pyramidally terminated crystals.

ACKNOWLEDGMENTS

The author wishes to thank A. J. Palmer for drawing his attention to this halo. G. A. Chapman of the San Fernando Observatory for assistance in digitizing the halo photograph.

* Present address, Space Physics Laboratory, Aerospace Corporation, P.O. Box 92957, Los Angeles, California 90009.

† Present address, Department of Astronomy, University of Texas, Austin, Texas 78712.

REFERENCES

1. E. Bruche and D. Bruche, "Über die Photometric von Sonnenringen," Meteorol. Z. **49,** 289–294 (1939).
2. D. K. Lynch, "Polarization models of halo phenomena. I: The parhelic circle," J. Opt. Soc. Am. **69,** 1100–1103 (1979).
3. G. P. Konnen, 1983, "Polarization and intensity distributions of refraction halos," J. Opt. Soc. Am. **73,** 1629–1640 (1983).
4. D. K. Lynch, 1983, "The 22° and 46° halos: observation and theory," in *Digest of Topical Meeting on Meteorological Optics* (Optical Society of America, Washington, D.C., 1983), Paper FA2.
5. N. K. Nikiforova, A. G. Pavlova, A. G. Petrushkin, V. P. Synkov, and O. A. Volkovitsky, "Aerodynamic and optical properties of ice crystals," J. Aerosol Sci. **8,** 243–250 (1976).
6. F. Pattloch and E. Trankle, "Monte Carlo simulation and analysis of halo phenomena," J. Opt. Soc. Am. A, **1,** 520–526 (1984).